Transient Optimization for the Betterment of Turbine Electrified Energy Management

Jonathan L. Kratz*, Dennis E. Culley†, and Julian Lehan‡
NASA Glenn Research Center, Cleveland, Ohio, 44135, U.S.A.

Gas turbine engine transients are associated with degraded compressor operability, which must be addressed by the engine control system and accounted for in the engine design. Failure to do so may result in events such as compressor stall/surge and combustor blow out. Transient operability concerns constrain the engine design and can result in sacrifices of efficiency and/or thrust responsiveness. The traditional approach to transient operability management is control logic that limits the fuel flow command. A companion paper presents a strategy for optimizing the transient fuel flow control logic taking into consideration transient operability and thrust responsiveness. The study covered here extends this idea to an electrified gas turbine engine that employs a power/energy management concept known as Turbine Electrified Energy Management (TEEM). TEEM uses an electric power system interfaced with the engine (hence the term 'electrified gas turbine engine') to further improve transient operability and alleviate associated design constraints. There can be costs associated with implementing TEEM in terms of power and energy requirements that impact the size of the electrical power system. However, the results of this study show that through optimization of the transient limit logic, power and energy requirements needed to implement TEEM can be significantly reduced. Among the conclusions that can be drawn from the results of the illustrative application covered herein are: (1) there is a reduction in the electric machine power requirement to manage operability during accelerations by 200 to 400 hp, and (2) power transfer from the low pressure spool (LPS) to the high pressure spool (HPS) is the most effective option for improving operability during decelerations, followed by the options of only injecting power on the HPS or only extracting power from the LPS.

I. Introduction

Aero engines must operate reliably over a wide range of conditions, both steady-state and transient. The transients are primarily associated with rapid changes in thrust/power demand. For many military applications (especially fighter aircraft) transient operation is an important consideration during engine and controller development given the relatively high potential for dynamic operation. In contrast, commercial aircraft mission profiles are constrained and predictable, which shifts the focus toward the minimization of component life usage during takeoff and landing transients, and toward the reduction of cruise fuel consumption [1]. Transient operability is a factor that not only impacts control design, but also the design of the engine itself. References [2] and [3] cover many of the challenges posed by transients and allude to how they constrain engine performance.

This paper is a companion to Ref. [4]. Reference [4] presents a strategy for optimizing the transient limit schedules of a gas turbine engine using a genetic algorithm. It then extends the use of the optimization strategy to update the transient limit schedules over the lifespan of the engine utilizing a reinforcement learning algorithm. Here, the same optimization strategy is applied to the same propulsion system, but with focus on the inputs from the electrical power system used to implement the Turbine Electrified Energy Management (TEEM) concept. In this paper, the response time and power system size trade space is investigated. In addition, a scheduled approach to implementing TEEM control is considered that utilizes results from the optimization to derive the schedules.

* Research Engineer, Intelligent Control & Autonomy Branch, AIAA senior member.
† Research Engineer, Intelligent Control & Autonomy Branch, AIAA senior member.
‡ Intern, Intelligent Control & Autonomy Branch, non-AIAA member.

In the context of this paper, transient operability will refer to the degree to which the compressors within the engine are susceptible to stall or surge during engine transients. This is often quantified by stall margin, but alternative metrics will be introduced and used in this paper. Reference [4] focused on the traditional means for handling transient operability issues by modifying the fuel flow input. The TEEM transient operability management control concept extends this idea by making active use of an electric power system to improve transient operability [5]. This idea is prompted by the integration of electric machines (EMs) and energy storage, as is inherent with EAP concepts such as those described in Ref. [6]. However, the idea could be applied to traditional engines in the near-term with the addition or modification of some components. The basic idea of the TEEM concept is to leverage EMs (motors/generators) interfaced with the engine shafts to apply torques that help the speeds of the engine shafts stay in-sync with the air flow such that off-incidence flow through the compressors is reduced. The compressors can be sensitive to the off-incidence flow and stall or surge can occur if the air flow and shaft speeds get too far out of sync. An energy storage element is included to allow power to be injected into or extracted from the shaft(s) as necessary. TEEM leverages the electrical power system as a set of additional actuators and provides an active means of improving transient operability rather than accepting the issue and simply managing it by limiting the fuel flow rate. Given this type of power management scheme, TEEM should significantly enhance the transient operability through the active minimization of the engine's excursion from its nominal operation. However, the benefit may come at the expense of adding electric power system components or increasing their size, as well as increasing complexity. Therefore, the optimization of acceleration and deceleration limit logic that limits the fuel flow to mitigate operability issues is important to assure that the net benefits associated with implementing TEEM are maximized. References [5, 7-11] provide additional information about TEEM.

The goal of this study is to optimize the acceleration and deceleration control logic in order to minimize variations from the steady-state operating line during transients. An expected byproduct of the optimization is less harsh transients in terms of metrics such as those associated with compressor operability. Benefits were demonstrated without TEEM in Ref. [4] and are considered in this study in conjunction with TEEM. The study seeks to obtain a fair approximation of the operability benefits gained from TEEM given that prior studies have not considered optimized fuel flow control logic to improve transient operability. Results are presented that quantify operability improvement vs. power system size trades for employing TEEM with and without optimization. The optimal results are also thought to be valuable for control law design, particularly for the electric machine inputs. Advanced optimal control techniques such as Model Predictive Control (MPC) [12] could be employed. However, such methods can be complex, computationally expensive, and relatively difficult to certify. Therefore, a simpler schedule-based method is considered and evaluated.

The approach for optimization entails wrapping a genetic algorithm optimizer around a nonlinear model of a conceptual advanced geared turbofan to derive the optimal control inputs for extreme transients. The form of the power input profiles is constrained to reduce the optimization search space and to make the derivation of a schedule-based control approach more amenable. This study will focus on sea level static (SLS) burst and chop transients and will consider a variety of different control strategies and engine health states.

The rest of the paper is organized as follows. Section II provides a brief description of the TEEM control strategy as it applies to this study. Section III provides a summary of the methods employed in Ref. [4] and how they are extended to the application of TEEM. Section IV and its sub-sections cover the results of various simulations and optimizations. Section V investigates a scheduled control approach for TEEM that leverages the optimization results. Finally, Section VI provides some summarizing remarks.

II. Turbine Electrified Energy Management Control

The purpose of TEEM is to tightly regulate the operability of a gas turbine engine system, particularly its compression system, to the benefit of the engine and the vehicle it propels. The primary focus of TEEM has been on improving transient operability of the compression system. Enabling tighter regulation of the operability during transients will alleviate constraints on the engine design, thus leading to design decisions that improve efficiency and/or reduce weight.

The AGTF30 [13] is an engine model of a conceptual advanced geared turbofan with technologies thought to be matured around the year 2035. It is capable of ~30,000 lb_f of thrust at SLS conditions. The engine features a compact core. Its primary actuators are the fuel flow rate input w_f, a variable bleed valve for stability, and a variable area fan nozzle. The model was updated with health parameters to model degradation of the turbomachinery components. The degradation model was taken from the Commercial Modular Aero-Propulsion System Simulation 40,000lb_f engine model [14]. This study will consider a new (NEW) engine and end-of-life (EOL) engine.

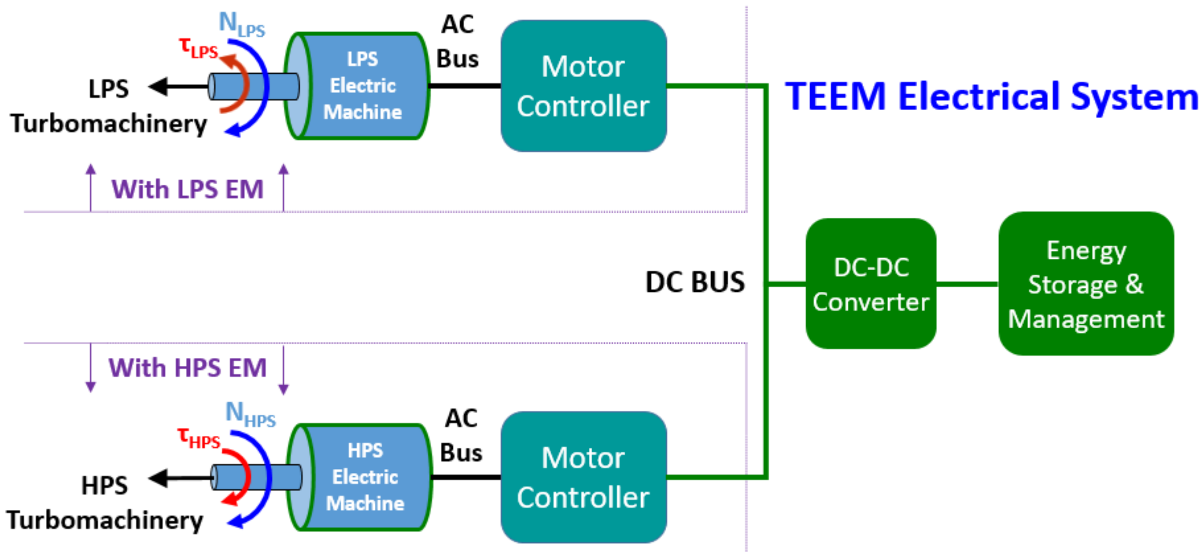

Figure 1. Schematic of a proposed electrical system architecture for TEEM. Power addition is depicted for the HPS EM while power extraction is depicted for the LPS EM [7].

The engine model was updated to include an electrical power system to implement TEEM. That work is described in Ref. [7] and the model from that study will be utilized in this study. The basic power system architecture is depicted in Fig. 1. In the figure, N represents a shaft speed in rpm and τ represents a torque applied by an EM. The power system consists primarily of 2 EMs and energy storage. One EM is interfaced with the High Pressure Spool (HPS) and the other is interfaced with the Low Pressure Spool (LPS). The HPS EM is 400hp with a nominal power extraction of 350hp. The LPS EM is 410hp and the energy storage system has an energy capacity of ~0.7kW-hr. The sizing was taken from the results of the study covered in Ref. [8]. The components are connected through a power transmission system that includes a DC-DC converter, a DC bus, and EM controllers (inverter/rectifier pairs). The electrical power system is modeled with the NASA-developed Electrical Modeling and Thermal Analysis Toolbox (EMTAT) software. EMTAT is a MATLAB/Simulink® based toolbox that is compatible with the Toolbox for Modeling and Analysis of Thermodynamic Systems (T-MATS) [15] used to model the engine. While EMTAT has a variety of blocks with different modeling approaches, the set of blocks utilized in this model utilize a power flow modeling approach.

References [5], [7], and [8] present observations on how to use the electrical power system to improve transient operability. References [7] and [8] outline control strategies for employing TEEM on the AGTF30 engine. A controller developed in that study will be utilized in part of the studies covered in this paper, comparing its performance with optimal results. In general, power addition to the HPS is helpful during accelerations. The additional energy applied with the HPS EM is supplied by the energy storage system. Power extraction from the LPS and power addition to the HPS tends to be helpful during decelerations. Both can be done by themselves or in combination. Since in-flight re-charging of the energy storage devices (ESDs) is envisioned to reduce ESD size and the on-ground charging burden, a 1-for-1 power transfer approach is thought to be the most beneficial approach during decelerations. This will help to reduce the size of the LPS EM and mitigate issues related to power/energy dissipation if the LPS EM were to extract more power than is applied by the HPS EM. It will also help to reduce the size of the ESDs compared to a situation in which the HPS EM applies more power during the deceleration than the LPS EM extracts.

The control strategy is summarized in Fig. 2. It consists of activation logic, a Proportional Integral (PI) controller, and a transition function that will encourage smoother transitioning between the transient and steady-state operating modes of the controller. The HPS EM controller seeks to achieve a corrected HPS speed that is corrected with engine inlet conditions. The HPS speed schedule is a function of the normalized w_f command[§]. The set-point schedule is derived from steady-state data and thus the idea is to keep the compressor operating near its steady-state conditions. Likewise, during decelerations the LPS EM controls the corrected LPS speed (also corrected to the engine inlet conditions). During decelerations, the power commanded for extraction by the LPS EM is input by the HPS EM. Due to losses in the power system, this will result in a small power draw from the ESDs, but it is essentially a power

[§] The set-point schedule will also vary with flight condition (altitude and Mach number) transfer from the LPS to the HPS. The activation logic utilizes information from the w_f controller to determine if the engine is accelerating, decelerating, or is at steady-state. The logic computes a normalized error based on the active w_f controller (whether it is the nominal corrected fan speed controller or one of its limiters). The normalized error is represented in Eq. (1) where X is the control variable and the subscripts "*SP*" and "*range*" refer to the set-point and the expected range of the variation of the control variable.

$$E_{norm} = \frac{X_{SP} - X}{X_{range}} \quad (1)$$

When the magnitude of the normalized error is above a defined threshold and the error value is positive, it indicates an acceleration. When the magnitude is above a defined threshold and the error value is negative, it indicates a deceleration. If the magnitude of the normalized error is below the defined threshold, it indicates steady-state operation. The transition function is a logistics function that varies between 0 and 1 and is a function of the normalized error. It is multiplied by the commanded EM torques prior to being sent through to the EMs.

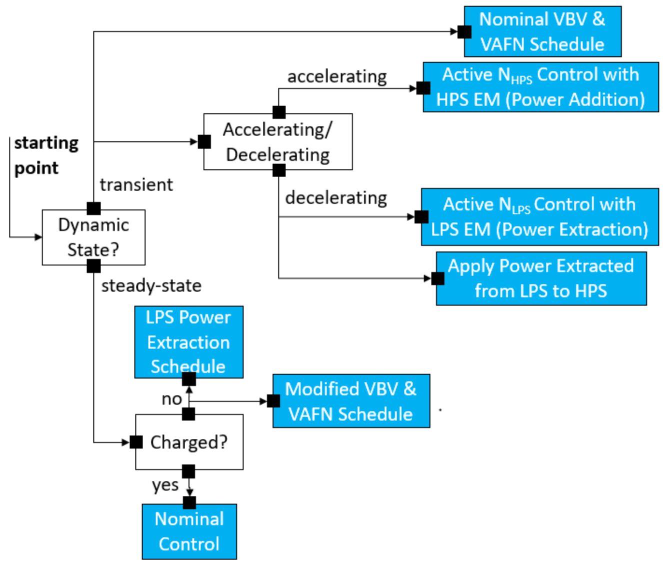

Figure 2. High level control logic for implementing TEEM. [8]

The engine model can use two different acceleration and deceleration limit schedules. The original acceleration and deceleration limit logic results in what will later be referred to as the "baseline w_f profile." In addition, a simplified acceleration and deceleration limit logic is defined that takes advantage of the EMs to simplify the logic. It essentially enforces a w_f ramp rate that results in a desired thrust response time. This option is referred to later as the "simplified w_f profile." Both the "baseline" and "simplified" acceleration schedules are considered later and compared with optimized w_f input profiles.

Some of the simulations conducted in this study will utilize the controller described above. Others will attempt to optimize the EM power/torque inputs for comparison. In cases where the EM power/torque inputs are optimized, they will still be under the same constraints as the controller mentioned above. Specifically, only the HPS EM will be utilized during accelerations. Power transfer will be the focus of decelerations. However, some attention will be given to the alternatives of only extracting power from the LPS or only adding power to the HPS. These approaches are described and illustrated in more detail in Refs. [7] and [8]. The HPS only option enables application of TEEM without an LPS EM. The sole use of the LPS during decelerations provides a regenerative braking benefit but it is only applicable when the power can be absorbed by the energy storage system, and it tends to be less effective than using EMs on both shafts.

III. Overview of the Transient Optimization Method

This section describes the optimization method outlined in Ref. [4] and notes discrepancies as applicable. The genetic algorithm employs functions of elitism, carry-over (replication), reproduction (crossover), and immigration. Mutations can be applied at various points in the algorithm. Random selection or rank-based selection are applied for member selection and other probabilistic processes. The algorithm has various options and noteworthy features. It enforces a fixed population size. It exploits the best solutions through adding mutations of the elite to the next generation. It has many options regarding how reproduction is handled. This includes flexibility for how many times a member of the population can participate in reproduction and the number of offspring a reproduction pair can produce per generation.

Reference [4] uses the genetic algorithm to manipulate the w_f input profile to maximize the fitness, f, of the solution on the basis of transient operability. The fitness function is given by Eq. (2).

$$f = \frac{1}{TSU} \tag{2}$$

TSU is the transient stack usage defined in Eq (3). *PR* is the pressure ratio in the simulation while PR_{SS} and PR_{stall} are the pressure ratios of the steady-state operating line and stall line at the same corrected flow rate W_c respectively.

$$TSU = max\left(\frac{PR - PR_{SS}}{PR_{stall} - PR_{SS}}\right) \times 100\% \tag{3}$$

For each optimization, the desired thrust response time is achieved by stretching or compressing the w_f profile through an iterative root solver. The thrust response time is defined as the time to reach 95% and 20% of the maximum thrust value during accelerations and decelerations respectively. The optimization is similar for defining the EM power inputs relative to the nominal power extraction. This is the power command for implementing TEEM to improve transient operability. The fitness function for determining the EM power commands is defined as a function of the integral of the deviation between the transient running line and the steady-state operating line, which will be referred to throughout this paper as the Transient Excursion Integral (*TEI*) as defined in Eq. (4).

$$TEI = \int \left|\frac{PR - PR_{SS}}{PR_{SS}}\right| dW_c \tag{4}$$

The *TSU* and *TEI* terms are illustrated in Fig. 3. To summarize, the w_f input profile is optimized to flatten the transient operating line and minimize the usage of the operability stack while the power input profile for the electric machines is optimized to reduce the excursion of the transient running line from the steady-state operating line. In this study, it can be noted that the corrected flow rates and pressure ratios plotted and used in this study are the unscaled map values.

The w_f input optimizations are leveraged from Ref. [4] so details for how that optimization is setup are not covered here. For the electric machines, the power input profile is defined by nine points between 0 and the maximum power. To simplify the input profile and make the derivation of a more practical schedule possible, the profile was constrained to start at full power at the beginning of the transient, remain there for some duration of the desired thrust response time, and then decrease monotonically until the power input returned to zero at the prescribed thrust response time. The variables in the optimizer include the fraction of the transient time spent at the maximum power command, *X*, and the nine values between 0 and 1, *Y*, that are used to define the change in power between each of the eight data points that define the power profile as its magnitude decreases from its maximum value to 0. The time of each data point in this portion of the profile is spaced evenly. The EM power is a function of *Y*.

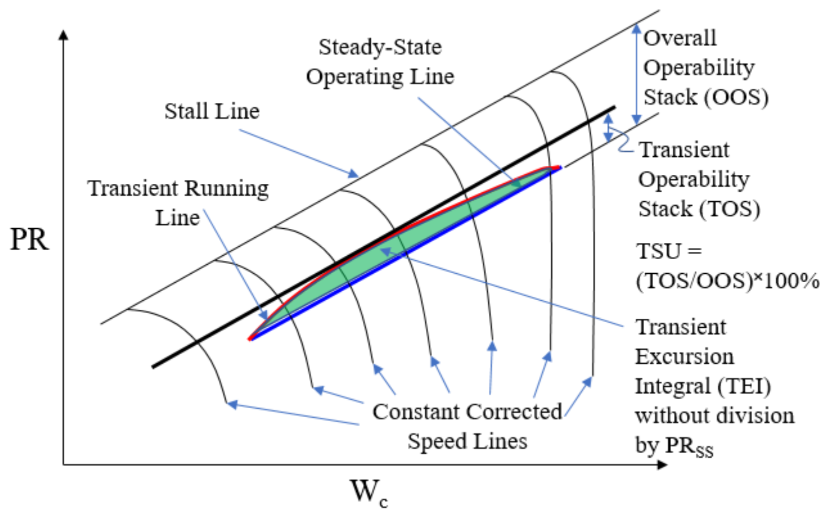

Figure 3. Illustration of TSU and TEI.

$$p_i = p_{i-1} - \frac{Y_i}{\sum_i Y_i} p_{max} \tag{5}$$

In Eq. (5), *p* is the EM power, *i* is the index of the time interval that the EM power change occurs over, and the subscript "*max*" refers to maximum power capability of the EM. For i = 1, the p_{i-1} term is equal to p_{max}. The optimizations consisted of simulations of the nonlinear AGTF30 model with different control inputs. A population size of 40 to 50 was utilized and 50 to 150 generations were typical.

IV. Transient Optimization

The transient maneuvers evaluated are full power range bursts and chops. A burst is characterized by the rapid increase in power/thrust and the chop is characterized by a rapid decrease in power/thrust. Section IV-A compares various simulation and optimization results to investigate the impact of the w_f profile on TEEM and its ability to improve transient operability. Section IV-B presents the results of various optimizations that quantify the operability benefits for various combinations of thrust response time and electrical system sizing constraints.

A. Impact of the Fuel Flow Rate Input

The baseline and simplified w_f profiles mentioned in Section II are considered along with two optimized w_f profiles. The first optimized profile is taken directly from Ref. [4] and does not consider TEEM. The other w_f input profile is optimized with the same method but utilized the TEEM controller from Ref. [7] while doing the optimization. Thus, four different w_f input profiles were considered, and various combinations of those w_f profiles with and without application of TEEM are simulated. All simulations were applied to a new engine. Figure 4 compares the w_f input profiles mentioned above while Fig. 5 shows the HPS EM power input profiles commanded by the TEEM controller. Figure 6 compares the thrust, F_n, response of the various simulations. A few observations are noteworthy. First, the power input to the HPS, with application of TEEM, results in a faster increase in thrust earlier in the transient. Second, the EM energy usage for TEEM, when using the optimized w_f input profiles, tends to be higher due to relaxed w_f profiles that produce a more relaxed corrected fan speed response (similar to the thrust response) that keeps the TEEM controller active longer. Finally, Fig. 7 illustrates how the transient running lines vary relative to each other. The *TSU*, *TEI*, and energy usage for each option is provided in Table 1. It should be noted that each option has the same thrust response time.

The operability results indicated by the *TSU* and observed in Fig. 7 suggests that TEEM implementation is significantly more effective with the optimized w_f input profiles. In fact, the *TSU* achieved without TEEM while using the optimized w_f profile is better than the *TSU* achieved with TEEM while using the baseline w_f input profile. With use of the optimized w_f input profile optimized without TEEM (from Ref. [4]), the transient running line is observed to nearly run along the steady-state operating line, essentially eliminating the transient stall margin stack. The optimization of the w_f profile conducted with application of TEEM (case 7 in Table 1) resulted in a very similar w_f input profile as the one optimized without TEEM (case 6 in Table 1). Only a slight improvement in operability was observed and nearly the same amount of energy was consumed. Based on this observation, it was assumed that the optimization of the w_f input without consideration of TEEM is sufficient and can be done a priori. This simplifies the process by eliminating the need for a TEEM controller prior to schedule design. It also eliminates the need to consider

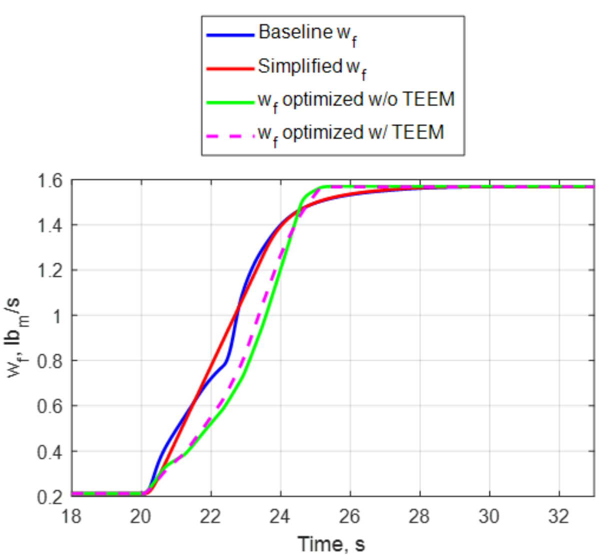

Figure 4. Fuel flow rate input profiles.

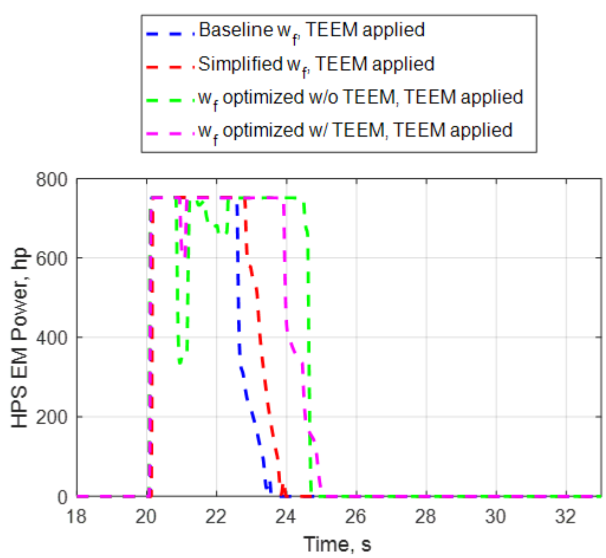

Figure 5. HPS EM power input profiles.

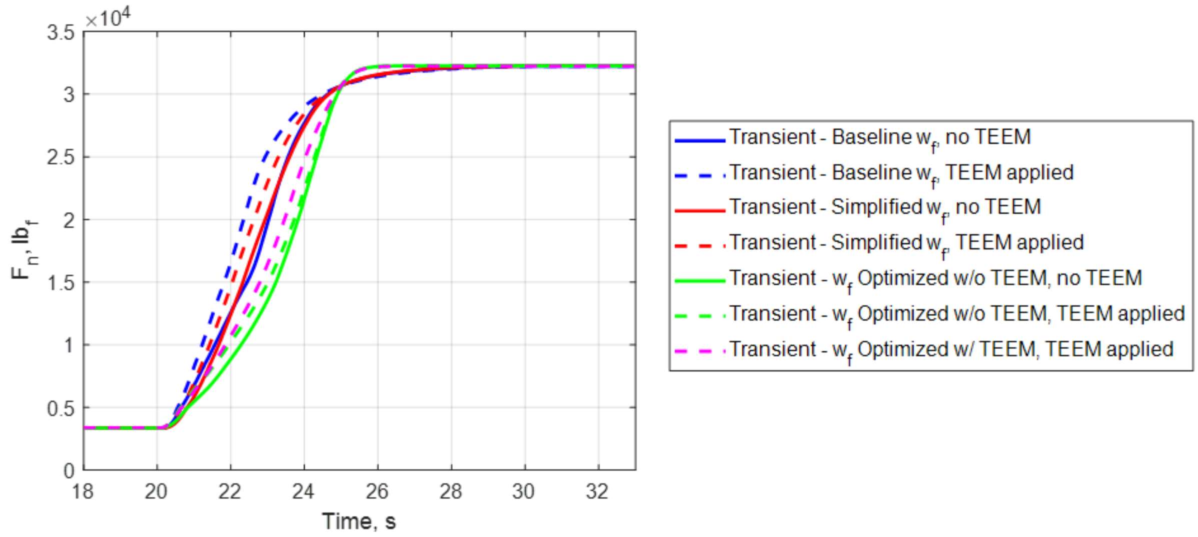

Figure 6. Thrust responses for various simulation options.

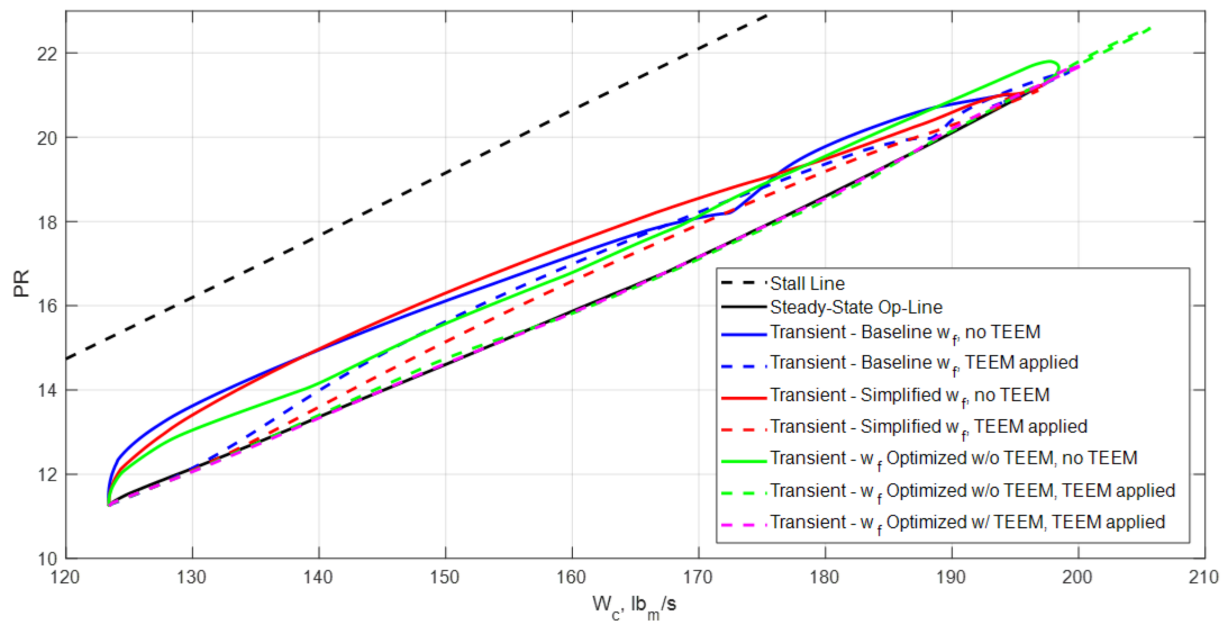

Figure 7. HPC map with transient running lines for various simulation options.

the coupling of the w_f and power input in the optimization, which would significantly impact the computational complexity of the optimization problem. This assumption appears to be reasonable for this application. The following sub-section will further investigate the trades between the choice of w_f input profiles.

Table 1. TSU, TEI, and Energy Usage Results

Case	**TSU, %**	**TEI, lb_n/s**	**Energy Usage, kW-hr**
1 - Baseline w_f, no TEEM	37.7	5.85	0
2 - Baseline w_f, TEEM applied	23.5	3.14	0.42
3 - Simplified w_f, no TEEM	37.9	5.98	0
4 - Simplified w_f, TEEM applied	16.0	1.89	0.49
5 - w_f optimized without TEEM, no TEEM	22.4	4.20	0
6 - w_f optimized without TEEM, TEEM applied	3.1	0.28	0.67
7 - w_f optimized with TEEM, TEEM applied	2.5	0.17	0.65

B. Response Time, Operability, and Electrical System Trades

Various optimizations were conducted to investigate the trade-offs between thrust response time, operability, and electrical system requirements for both accelerations and decelerations. Due to limited time and computational resources, the number of optimizations were limited and priorities had to be imposed. Optimizations primarily focused on defining the trade space for an EOL engine with the optimized w_f input profile from Ref. [4]. Additional optimizations were conducted for a NEW engine with the optimized w_f input profile and an EOL engine with the baseline w_f input profile. These additional optimizations were only conducted at the extremes of the investigated trade space to bound the results. For decelerations, alternative TEEM approaches were also investigated. The primary analysis captured by the optimizations described above were conducted assuming a power transfer from the LPS to the HPS. However, additional optimizations were conducted for scenarios in which only the LPS EM was used to extract power, or only the HPS EM was used to input power. Both sets of optimizations assumed an EOL engine and were only performed along the edges of the investigated trade space.

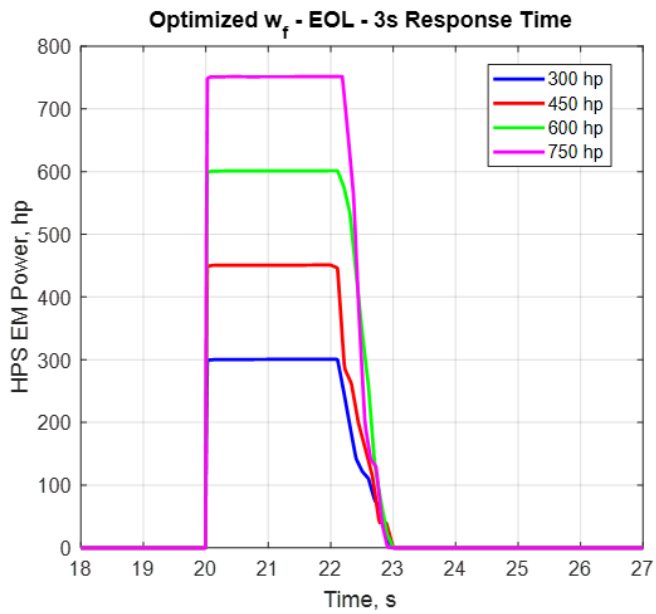

Figure 8. Example of optimized power input profiles for an EOL engine with the optimized fuel flow rate input.

The investigated trades space considered acceleration thrust response times of 3 to 5 s. The HPS EM power capability ranged up to 750 hp. For decelerations, the range of thrust response times was 7 to 11 s. The power range extended up to 500 hp and could represent either a power transfer, an extraction from the LPS, or an injection to the HPS, as applicable. Contour plots are used to present the data and “x” markers indicate the response time and EM power level combinations for which data was collected. This should be considered before making inferences about the data at other locations in the sparsely populated trade space. Accelerations will be considered first followed by decelerations. This section will summarize results from the study. Supplementary results showing the impact of different factors, as viewed on compressor maps, are presented in the Appendix.

Figure 8 provides examples of the optimal solutions for the power input profiles. Specifically, these results are for a 3 s thrust response during an acceleration with an EOL engine while applying the optimized w_f profile. In general, the profiles remained at the maximum power capability for most of the transient before tapering to zero.

Figures 9 and 10 show the variation of *TSU* and *TEI* through the trade space for accelerations, respectively. Figures 9a and 10a show the variation for an EOL engine with the optimized w_f profile. Figures 9b and 10b show a similar contour plot for a NEW engine and Figures 9c and 10c show similar contour plots for an EOL engine with the baseline w_f profile. The 3 contour plots share the same color map to aid comparison. To further aid in the analysis of the

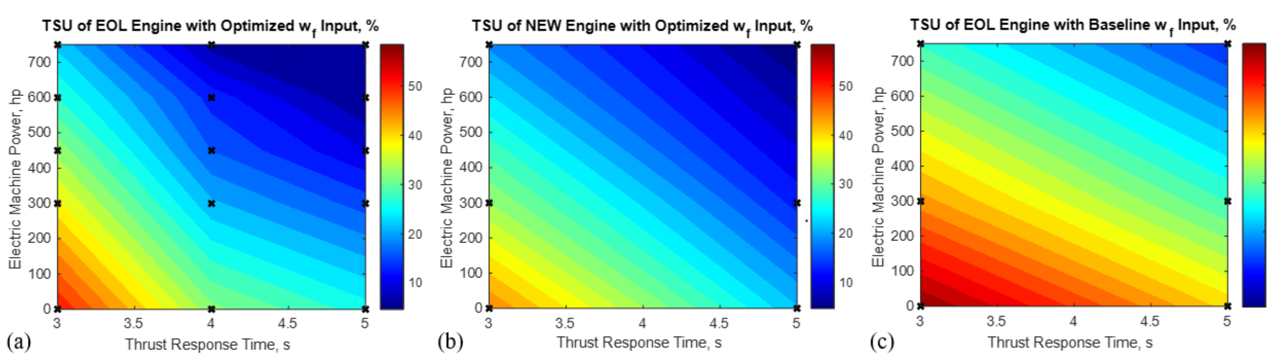

Figure 9. TSU contour plots for acceleration transients.

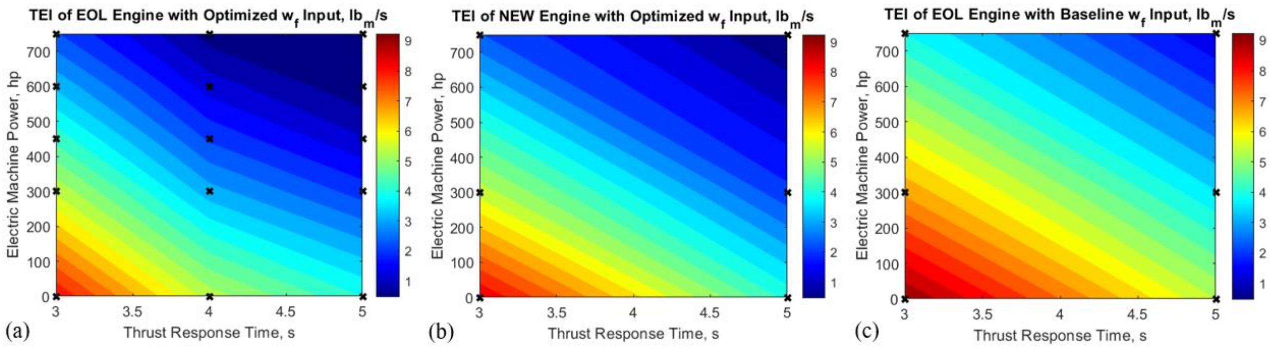

Figure 10. TEI contour plots for acceleration transients.

optimization results, Figs. 11a and 11c compare the *TSU* and *TEI* results for an EOL engine when the baseline and optimized w_f profiles are used. These results are for a 5 s thrust response time. In addition, Figs. 11b and 11d show the *TSU* and *TEI* results with the optimized w_f profile for different thrust response times. *TSU* and *TEI* are most favorable for higher thrust response times and higher EM power levels. Both metrics are improved significantly through the response time and power capability trade space by using the optimized w_f profile. For example, Fig. 11a indicates that the optimized w_f profile achieves the same *TSU* as the baseline w_f profile with 300 – 400 hp less. Put another way, for the same power capability, ~12% less of the overall operability stack is utilized. When considering *TEI*, it appears that about 200 – 300 hp can be saved by using the optimized w_f profile as opposed to the baseline. The results shown in Figs. 9 - 11 also demonstrate a growing rate of operability degradation as the thrust response time decreases, and this infers a growing requirement on the EM power capability to achieve a given operability margin. While an additional 150 -200 hp may be required to achieve the same *TSU* for a 4 s response vs. a 5 s response, an additional ~400 hp is required for a 3 s response vs. a 4 s response. Another observation is that while *TSU* decreases for a NEW engine compared to an EOL engine, *TEI* is very similar. *TSU* decreases largely because the steady-state operating line tends to shift toward the stall line as the engine degrades. The *TEI* metric suggests that the variation from the steady-state operating line remains consistent throughout the engine's life and the transient running lines in Fig. 27 of the Appendix help to illustrate this.

Figure 12 shows a contour plot of the energy usage during an acceleration transient. The energy increases primarily with power level, but it is also influenced by an increase in the thrust response time. Figures 13 and 14 seek to quantify

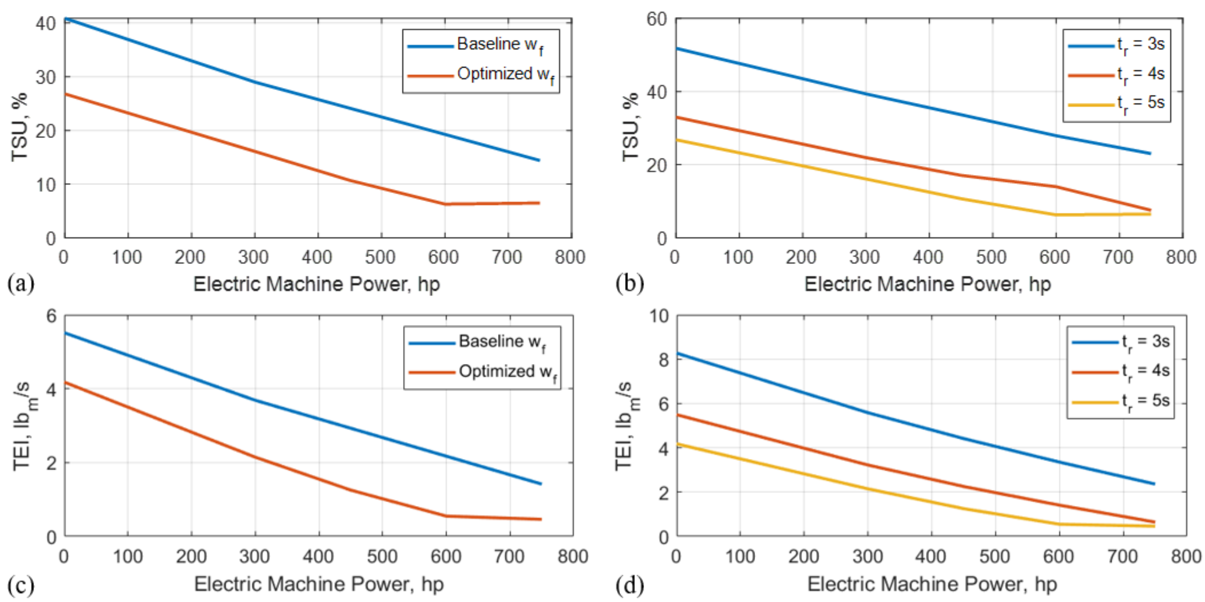

Figure 11. *TSU* and *TEI* results for comparing the impact of the w_f profiles and thrust response time for an EOL engine. (a) and (c) are results for a 5s thrust response demonstrating the impact of the w_f profile. (b) and (d) show the impact of the thrust response time with the optimized w_f profile.

the effectiveness of the electrical power system in improving transient operability by plotting the ratio of the *TSU* improvement from the result without TEEM and the EM power capability or energy usage, respectively. Figure 13 illustrates that a faster response provides more room for improvement and greater effectiveness of the electrical power system. The contour line in Fig. 14 tends to run relatively vertical and slightly from the top left to the bottom right. This indicates that the EM size has relatively low impact on the energy efficiency of the power system. If anything, the application of a small amount of power is slightly more effective per unit of energy than the application of a lot of power. The metric is driven more so by the thrust response time. A conclusion from this observation is that the choice of EM power level is likely more critical unless the energy density of the energy storage system is significantly less than the power density of the EMs on a relative basis. In general, the power system is more effective for its capability at lower EM power capabilities and lower thrust response times. For a 5 s thrust response time goal, for an EOL engine with the optimized w_f profile, a HPS EM power level of 450 – 600 hp seems reasonable. A lower power level will not experience additional benefits while a higher power level will encounter rapidly diminishing returns.

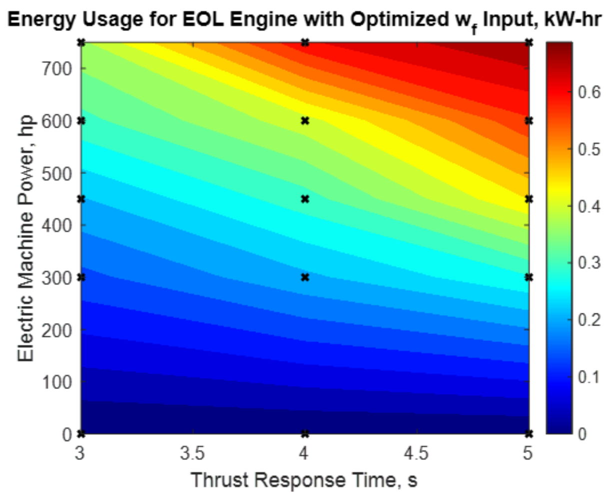

Figure 12. Energy usage for an EOL engine using an optimized w_f profile.

The remainder of this section will focus on the deceleration optimization results. Examples of the optimized power input profiles are shown in Fig. 15 for each deceleration strategy and Figs. 29 - 32 in the Appendix provide examples of the transient running lines on the Low Pressure Compressor (LPC) map. The plotted profiles consider an EOL engine and an 11 s thrust response time. The optimization with higher maximum EM power tends to quickly reduce

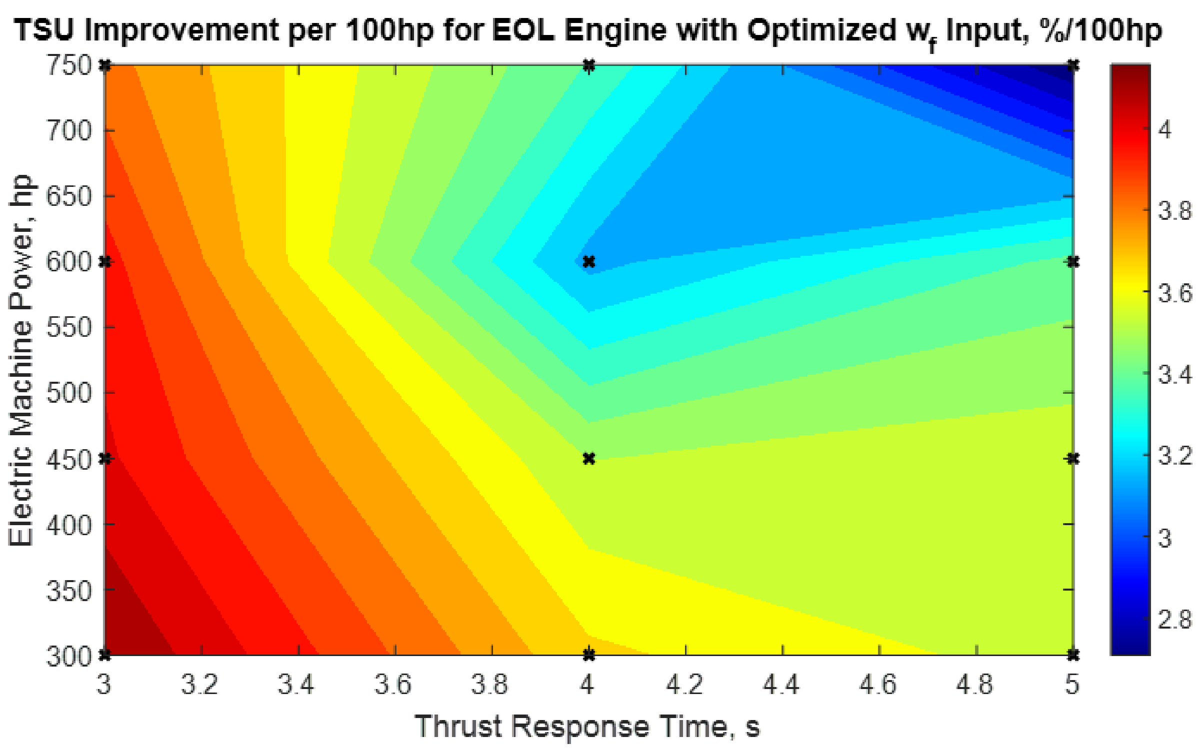

Figure 13. TSU improvement per 100 hp for acceleration transients.

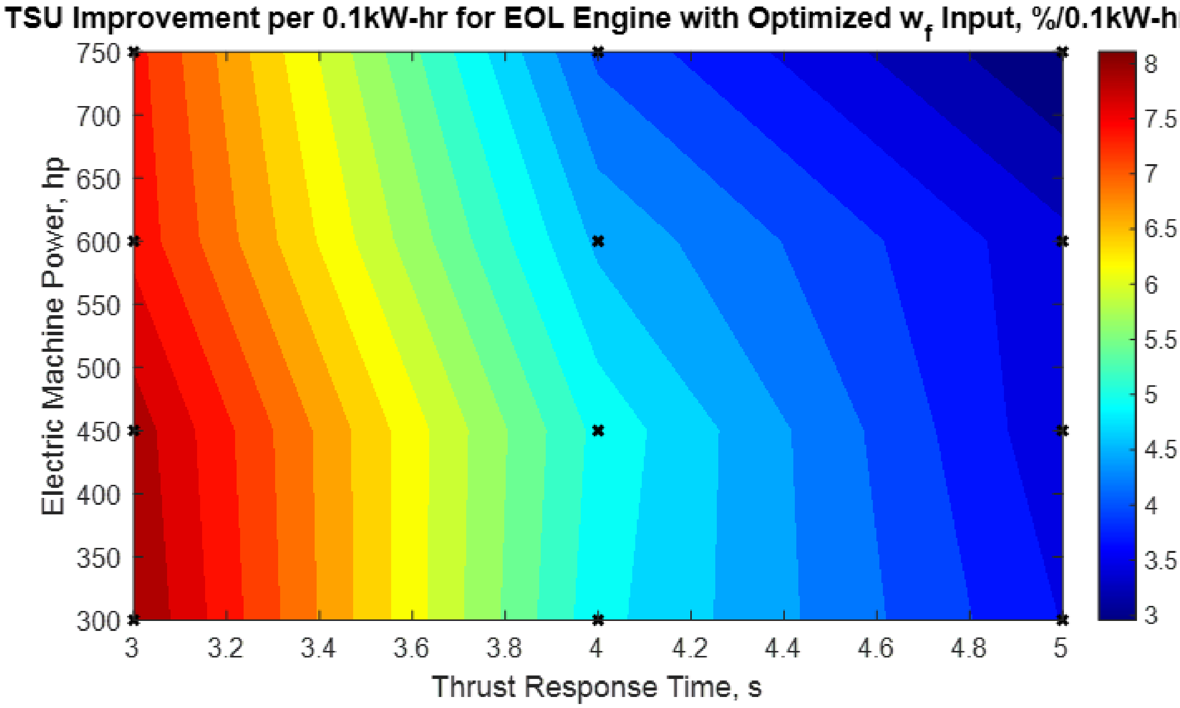

Figure 14. TSU improvement per energy usage for acceleration transients.

the power input to ~150hp near the start of the transient when both EMs are utilized. This indicates that a power transfer much above 150hp is not helpful. The profiles that only consider use of one of the EMs (Figs. 15b and 15c) do show a benefit to increasing the magnitude of the power injection or extraction during the first half of the transient. This portion of the transient occurs before the "kink" in the LPC operating line that corresponds to where the variable bleed valve starts to open to manage the stall margin. This feature can be seen in Figs. 29 - 32 of the Appendix in the zoomed in area. Still, there is a sharp drop in the magnitude of the power from 500 hp to ~300 hp with the HPS only and ~350 hp with the LPS only. In general, the power input profiles indicate that the TEEM control strategy employed in Refs. [7] and [8] might be more aggressive than necessary and the power system sizing recommendations were overly conservative. Reference [8] recommended 410 hp of power transfer or 610 hp of power extraction from the LPS if only it were used. The discrepancy could be partly due to control strategy, but the choice of operability measure is likely the dominant factor, as the minimum stall margin was the metric used for judgements made in Ref. [8].

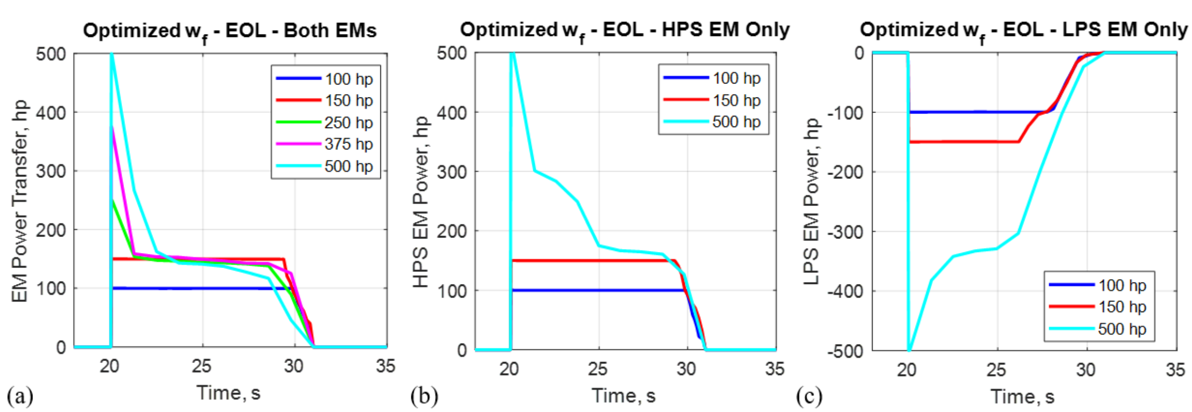

Figure 15. Optimized EM power profiles for 11s deceleration transients. The results consider an EOL engine with the optimized w_f input profile. (a), (b), and (c) show results for the different control strategies.

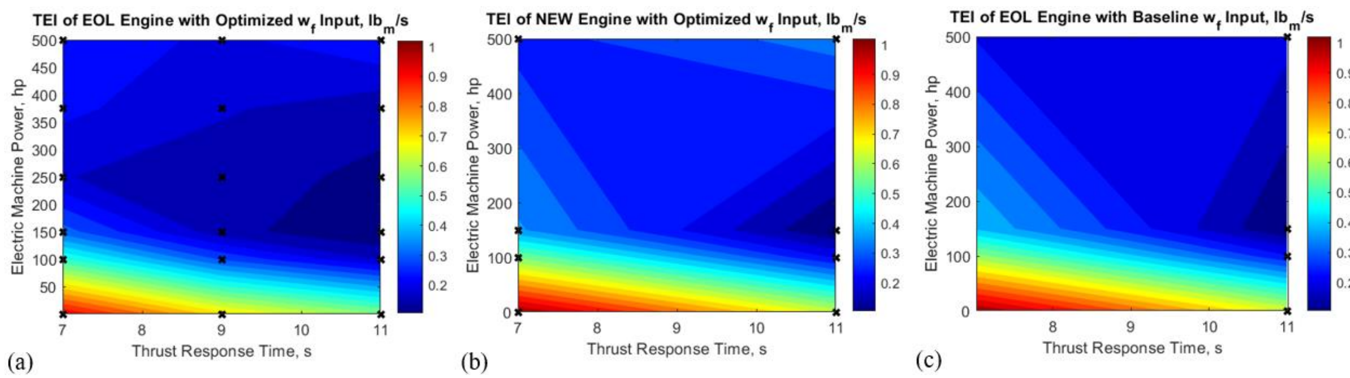

Figure 16. TEI trade space results for decelerations.

Figure 16 shows the variation of *TEI* throughout the response time and power level trade space. These results demonstrate that nearly all the benefit is achieved with ~150 hp of power transfer for an 11 s transient. For faster transients some additional power is beneficial. A notable feature in the results is that *TEI* will hit a minimum with respect to the EM power level and begin to increase for a given response time. This is because the initial increase in power will push the operating point below the steady-state operating line at the beginning of the transient, as can be observed in Fig. 31 in the Appendix. While this initial movement of the operating line downward can help to reduce deviation from the steady-state operating line later in the transient, it creates its own deviation that eventually becomes counter-productive as measured by the *TEI* metric. The results are similar for a NEW engine and an EOL engine with the baseline w_f input profile as seen in Figs. 16b and 16c. In both cases, *TEI* is slightly higher than with the EOL engine with the optimized w_f input profile. This result demonstrates the positive impact of the optimized w_f profile and the consistent impact of TEEM over the lifespan of the engine. Figure 17 shows the variation of *TEI* with respect to power for the different control strategies. This subset of the results is for an EOL engine with the optimized w_f profile and an 11 s thrust response time. The most

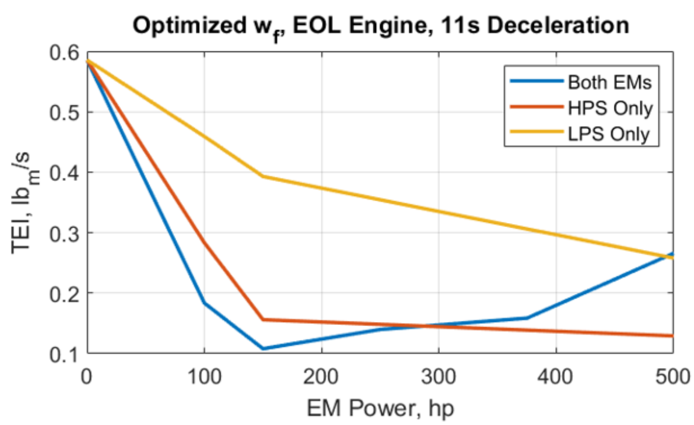

Figure 17. Comparison of *TEI* results based on control strategy.

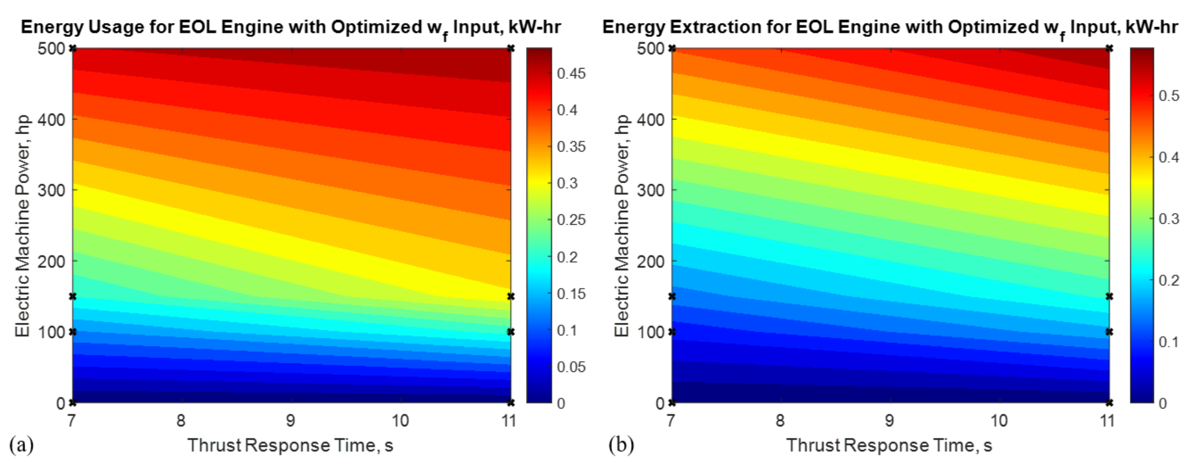

Figure 18. Energy usage/extraction during decelerations. (a) shows the energy usage when only the HPS EM is used and (b) shows the energy extraction when only the LPS EM is used.

interesting results are found between power levels of 0 to 150 hp, for which simulations were conducted at 0 hp and optimizations were conducted at 100 hp and 150 hp. Roughly speaking, to achieve the same *TEI*, the magnitude of power transfer using both EMs is ~75% of the power injected with only the HPS EM and ~33% of the magnitude of

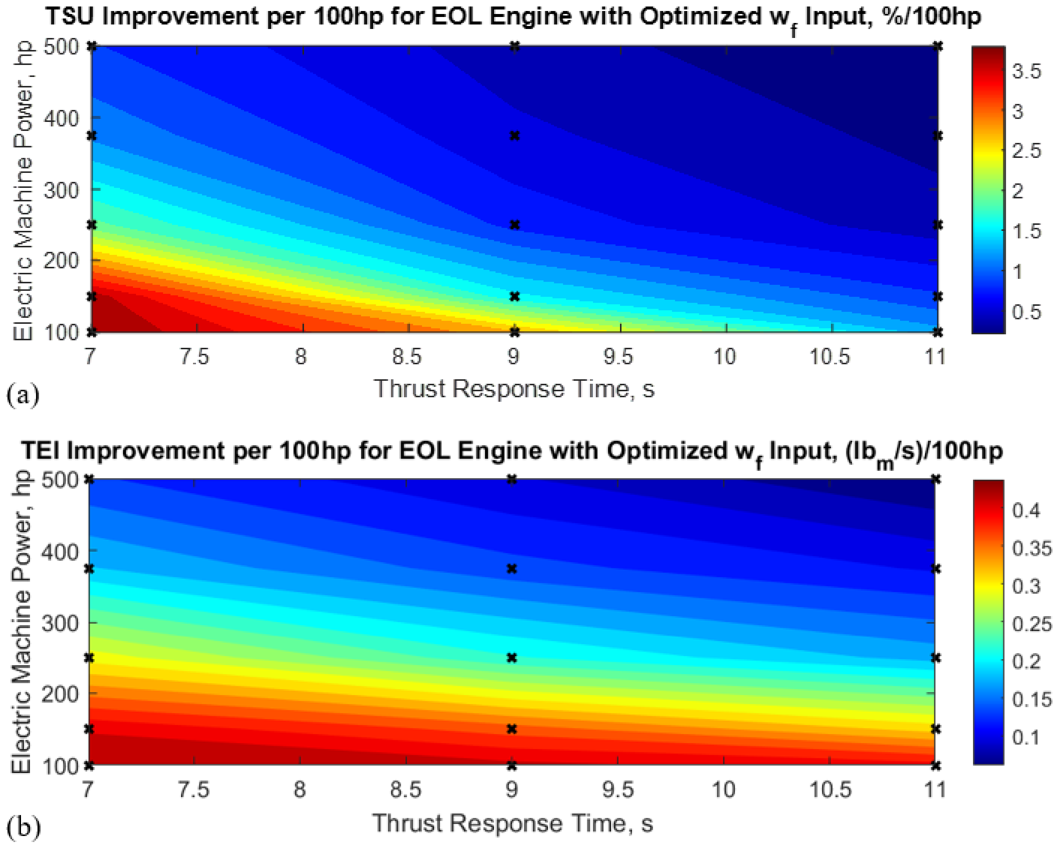

Figure 19. *TSU* and *TEI* improvement per 100 hp for and EOL engine with the optimized w_f input profile.

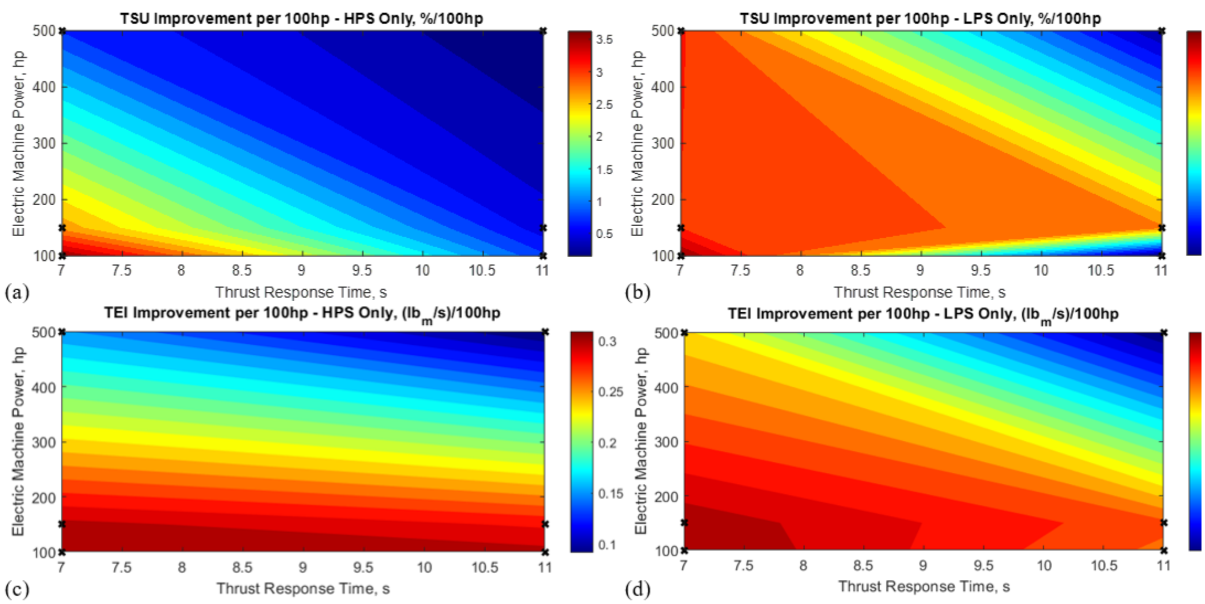

Figure 20. *TSU* and *TEI* improvement per 100 hp for and EOL engine with the optimized w_f input profile. (a) and (c) consider using the HPS EM only while (b) and (d) only consider use of the LPS EM.

power extracted when only using the LPS EM. Thus, the LPS EM size can be greatly reduced by using power transfer as opposed to just power extraction from the LPS. In addition, power injection on the HPS is more effective than power extraction from the LPS.

Figure 18 shows the energy usage and extraction for the HPS only and LPS only strategies, respectfully. Figure 19 shows the *TSU* and *TEI* improvements per 100 hp of EM when transferring power. The power specific improvement is highest at lower thrust response times and lower EM power capabilities. The same set of results is shown in Fig. 20 for when only the HPS EM is used or only the LPS EM is used. The results reinforce the claims made previously about the effectiveness of each strategy relative to one another.

V.TEEM Scheduled Control Approach

This section uses the optimization results to derive control schedules for implementing TEEM. These schedules would replace the closed-loop controller proposed in Refs. [7] and [8]. To demonstrate the idea, some of the optimization results were utilized to derive power schedules for commanding the two EMs during transients. In particular, the results from optimizations with the optimized w_f input profile and EOL engine were used. For accelerations, the 5s response time results were used while the 11s response time results were used for decelerations. These response times were chosen due to their proximity to the response times of the original AGTF30 model. The HPS EM and LPS EM power inputs for TEEM were limited to a magnitude of 450 hp and 150 hp respectively. The power schedules were defined as functions of the error between the set-point and sensed values of the corrected fan speed. This would imply that the w_f limit controllers would need to be set-point governors rather than directly commanding w_f. The schedule is plotted in Fig. 21. The acceleration and deceleration schedules were derived from the optimization results and are plotted in Fig. 22 where *RU* is the ratio unit and is equal to the w_f command divided by the static discharge pressure of the High Pressure Compressor (HPC).

The transient engine power level input profile shown in Fig. 23 was applied in simulation to the scheduled approach as well as the original closed-loop PI controller. Both control approaches utilized the same w_f controller and model settings other than the difference in TEEM control implementation. Figure 24 shows the power input for both methods. Figure 25 shows the movement of the operating point on the HPC and LPC maps. In this example, the results for the two methods are very similar regarding EM usage and operability improvement. It is noted that the tendency of the EM power to saturate may make the results for these methods look more similar than they would otherwise. Overall, the results demonstrate the

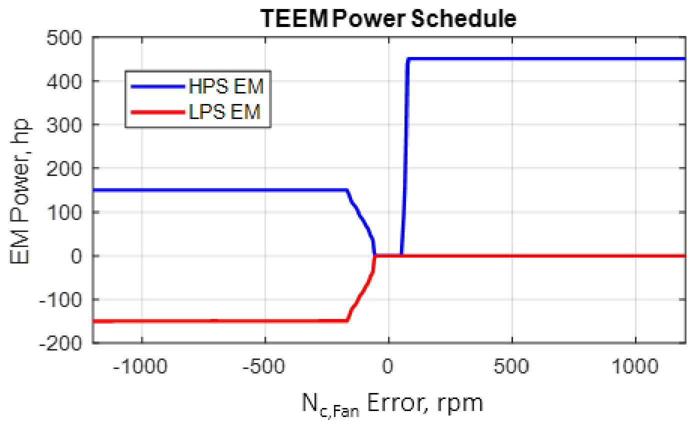

Figure 21. TEEM Power Schedule.

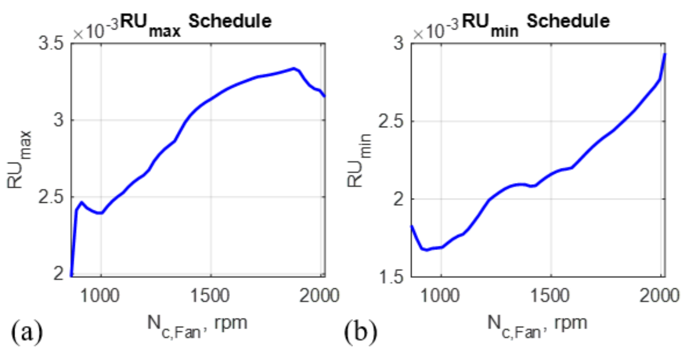

Figure 22. Acceleration and Deceleration Schedules.

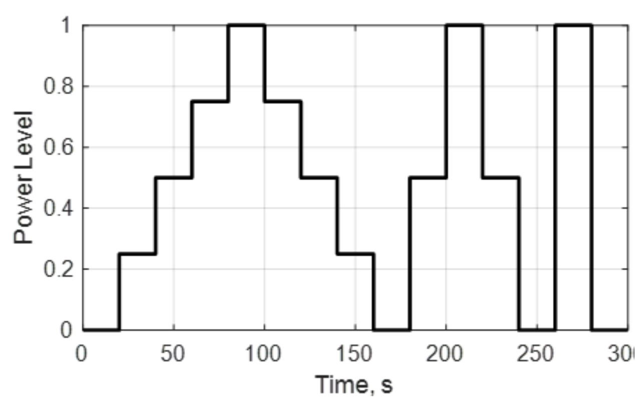

Figure 23. Engine power level command. Idle is 0 and full power is 1. The power level scales with thrust.

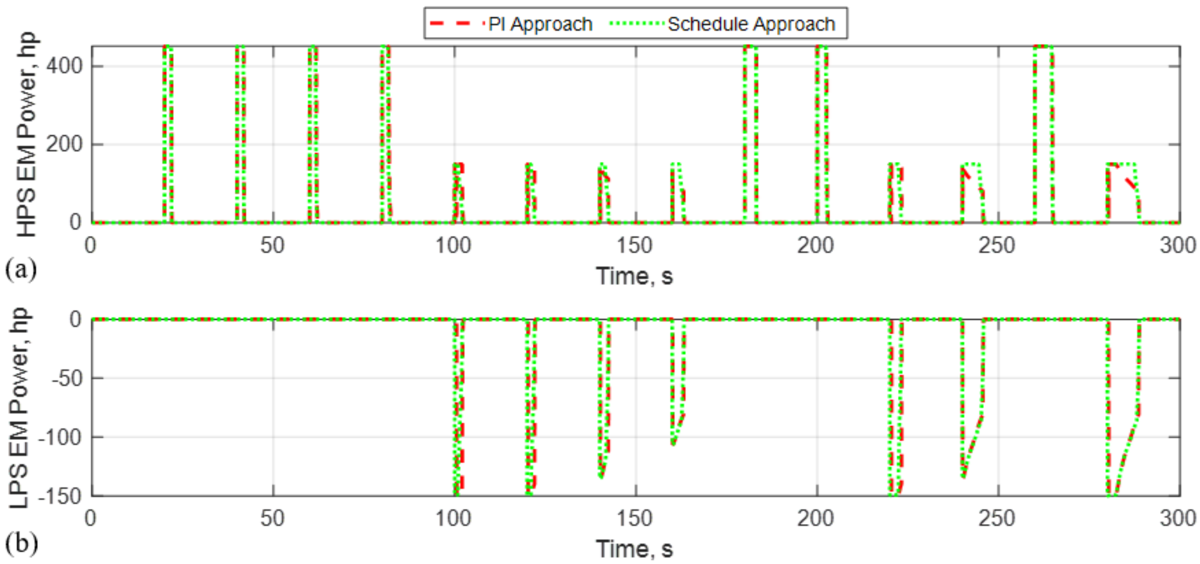

Figure 24. EM power inputs for the PI approach and the scheduled approach.

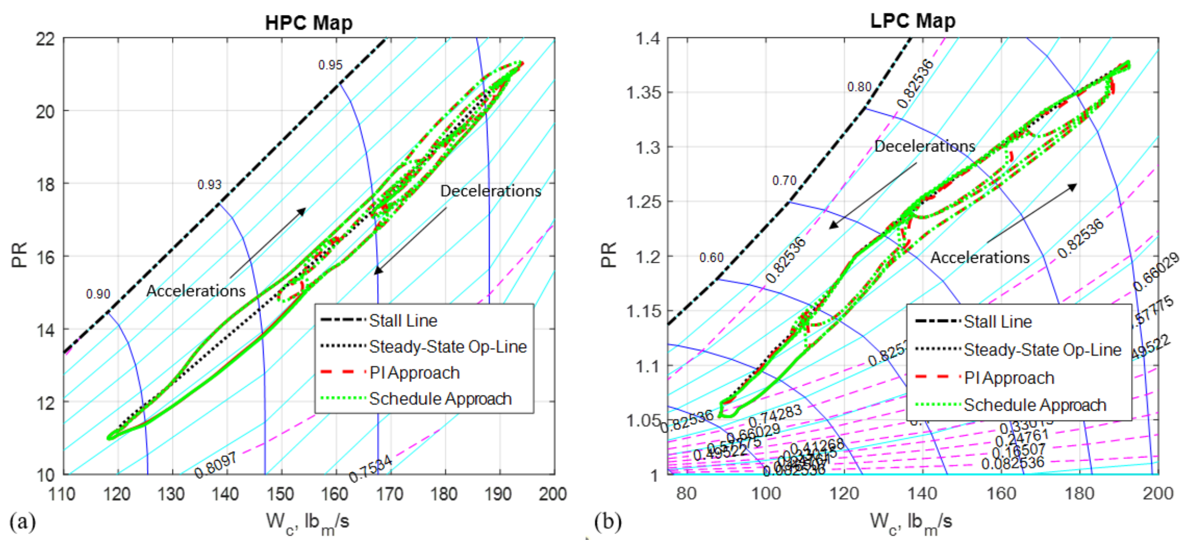

Figure 25. Compressor maps with transient running lines for the engine power input in Fig. 23.

feasibility of the scheduled-based approach and the near optimality of the original PI control approach. An advantage to the schedule-based approach is its simplicity. Not only is it an open-loop schedule, it also eliminates the need for activation/deactivation logic to determine when to apply torque with the EMs. Furthermore, it is not dependent on using the w_f command or a measurement/estimation of the w_f in the control law. Thus, it removes a source of error that could impact the controller commands.

VI. Conclusions

An approach for optimizing control inputs for an electrified gas turbine engine has been demonstrated. The approach leverages optimization techniques to optimize the fuel flow input profile to minimize the utilization of the transient operability stack, and the same techniques are applied to optimize electric machine (EM) power inputs such that the deviation of the transient running line from the steady-state operating line is minimized. Trade space analysis has been conducted to investigate the impact of various factors including operability, thrust response time, EM power level, energy usage, engine degradation, and use of an optimized fuel flow input profile versus a baseline profile. The results illustrate a significant operability improvement with the optimized fuel flow input profile, which improves the operability benefits of Turbine Electrified Energy Management (TEEM). In one case, it was shown that the optimized fuel flow input profile resulted in a 12% improvement in transient stack usage during acceleration transients. This enables a significant reduction in power system size to achieve similar transient operability. In the application covered in this paper, the High Pressure Spool (HPS) EM power can be reduced by approximately 200 to 400 hp, which also leads to a reduction in energy storage requirements. For decelerations, it was observed that power transfer from the Low Pressure Spool (LPS) to the HPS is most effective at improving transient operability. However, if only one EM could be utilized, power injection to the HPS is more effective than power extraction from the LPS. Results from an analysis such as this can be used to guide electrical system sizing decisions for implementing TEEM. Study results were used to derive a schedule-based control approach for implementing TEEM. This approach has been tested and compared with a closed-loop control approach that was proposed in a prior publication. The two methods yield similar results while the schedule-based approach is simpler and more predictable in operation. Future work may include the further exploration of the schedule-based control approach for implementing TEEM in other applications.

Appendix

This section includes various plots to provide supplemental illustration of the trade space evaluation. Figures 26 - 28 show acceleration transients while Figs. 29 - 32 show deceleration transients.

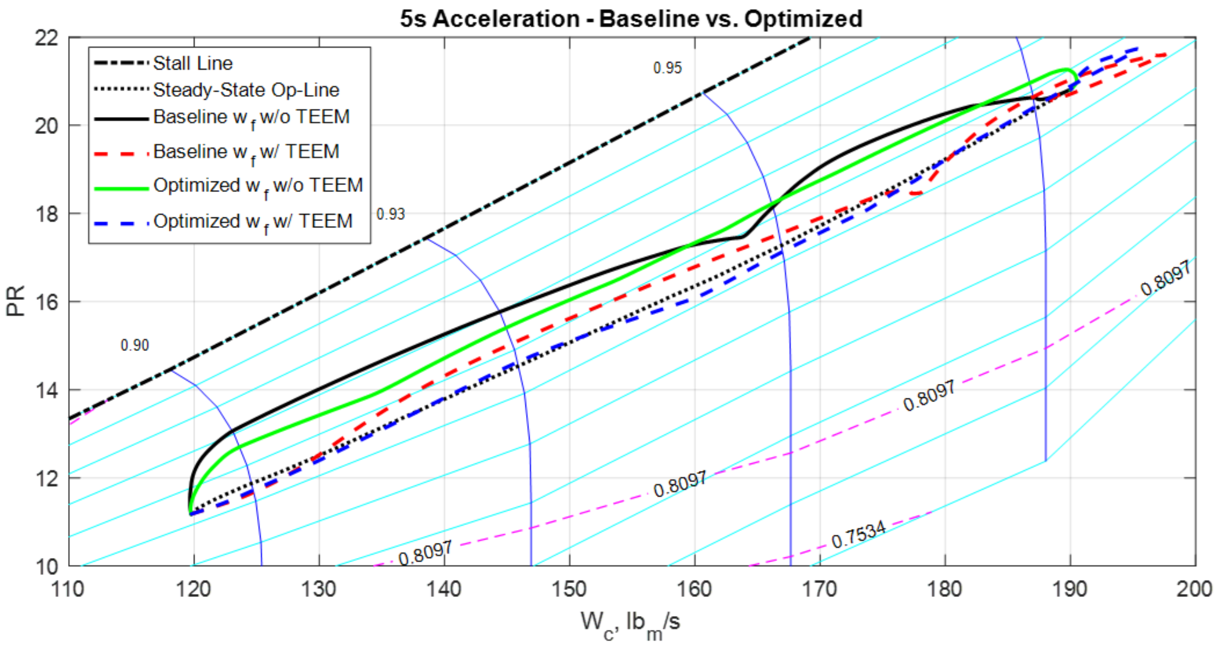

Figure 26. HPC map for a 5s acceleration transient with an EOL engine. Transient running lines are shown for simulations with the baseline w_f input profile and the optimized input profile, both with and without TEEM.

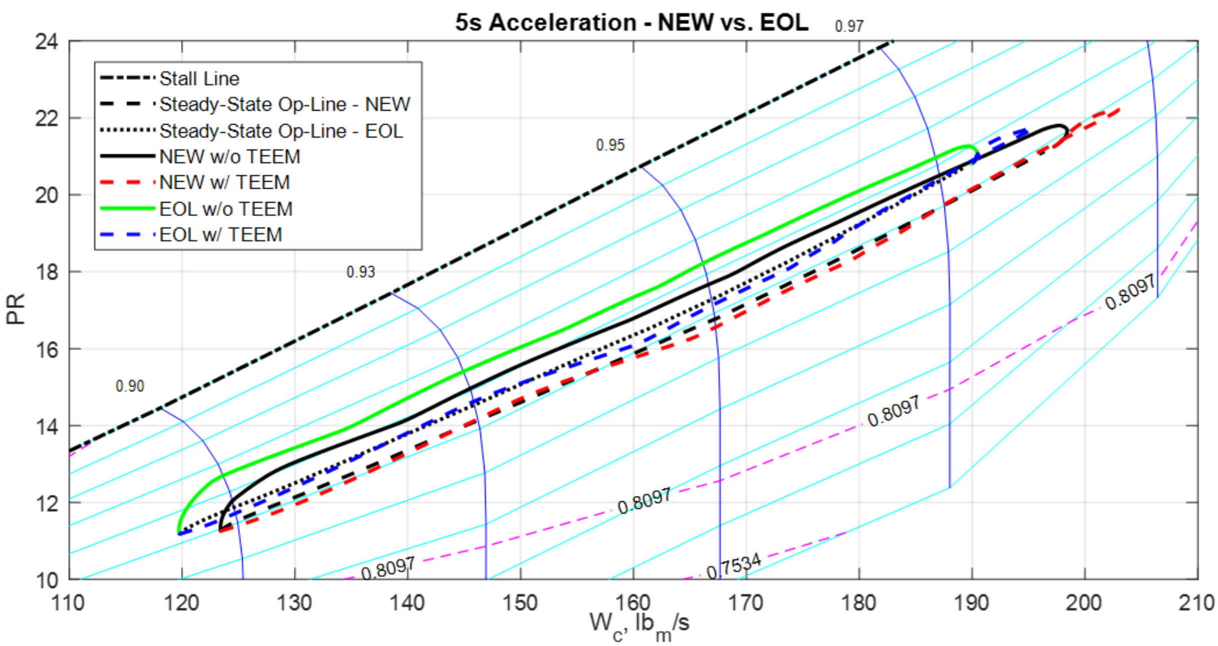

Figure 27. HPC map for a 5s acceleration transient and use of the optimized w_f input profile . Transient running lines are shown for a NEW and EOL engine with and without TEEM.

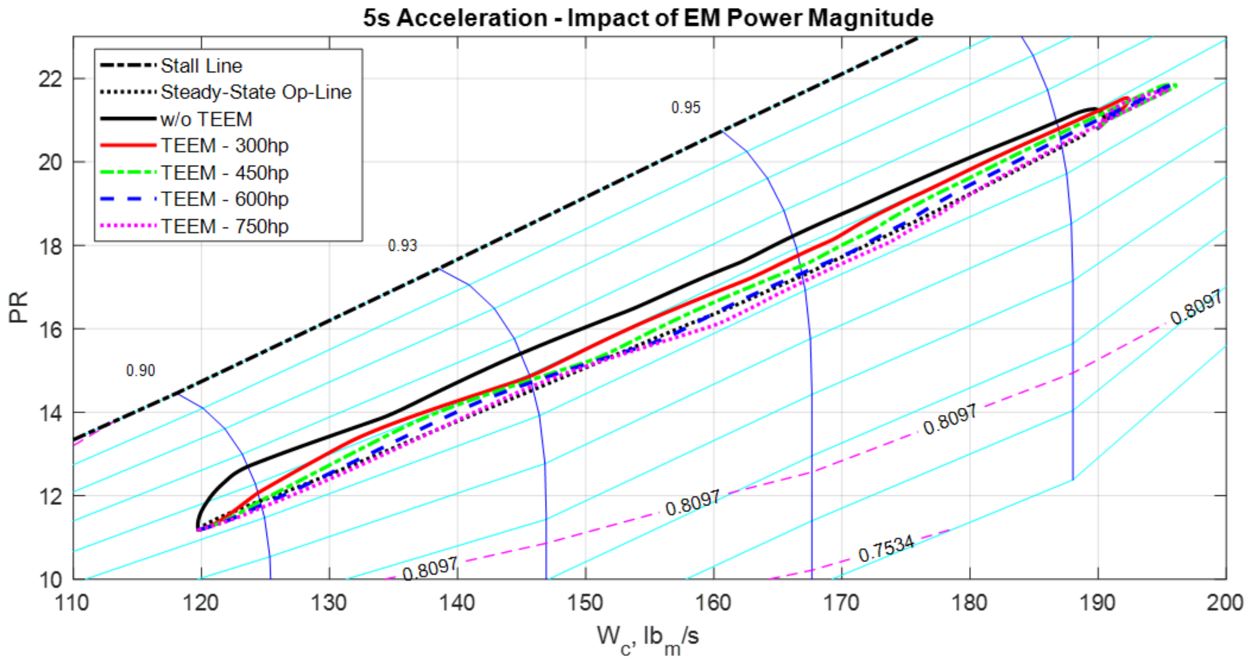

Figure 28. HPC map for a 5s acceleration with an EOL engine and use of the optimized w_f input profile . Transient running lines are shown for different HPS EM power levels.

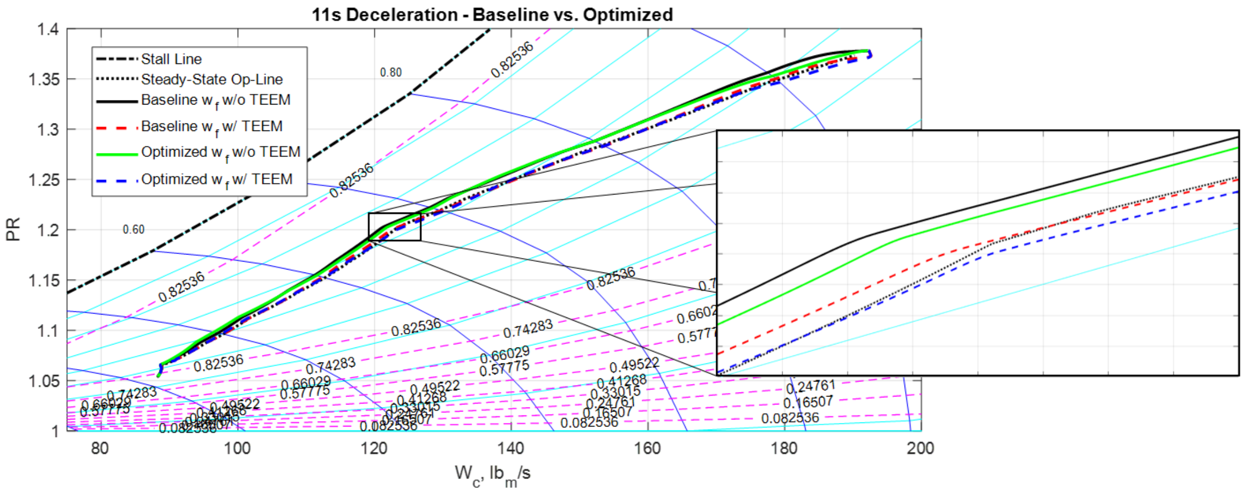

Figure 29. LPC Map for an 11s deceleration transient with an EOL engine and a maximum of 150 hp of power transfer. Transient running lines are shown for simulations with the baseline w_f input profile and the optimized input profile, both with and without TEEM.

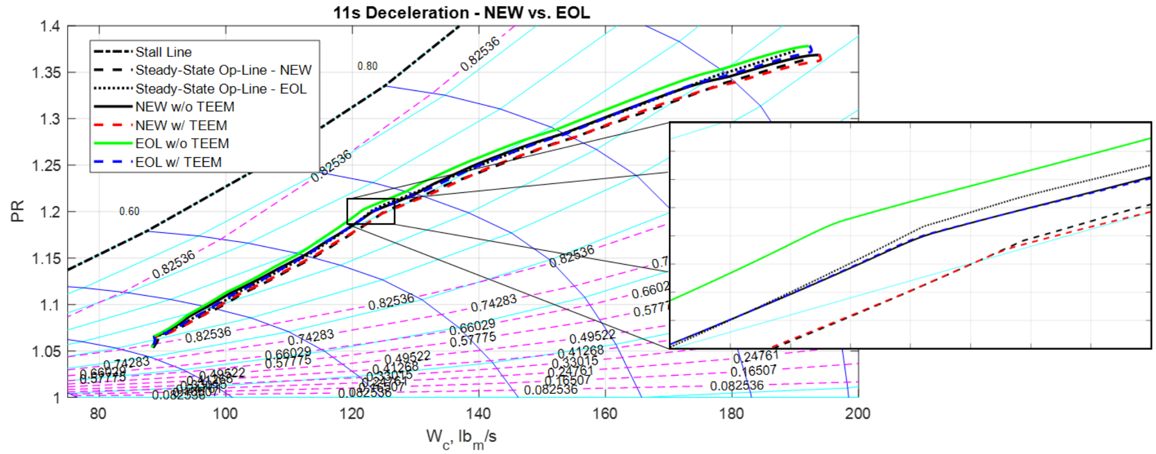

Figure 30. LPC Map for an 11s deceleration transient with an EOL engine and a maximum of 150 hp of power transfer. Transient running lines are shown NEW and EOL engines, both with and without TEEM.

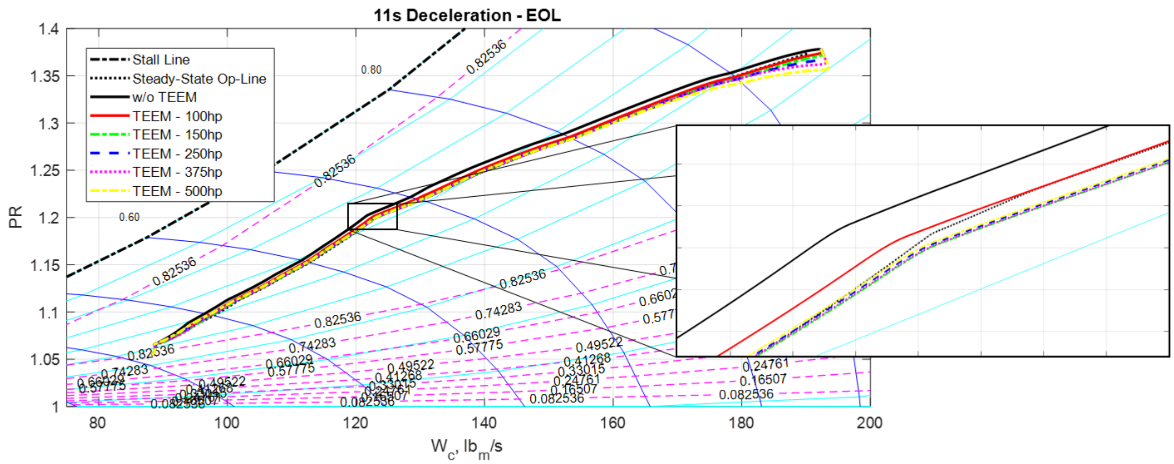

Figure 31. LPC map for an 11s deceleration transient with an EOL engine and both EMs being used when applying TEEM. Transient running lines are shown for varying levels of power transfer.

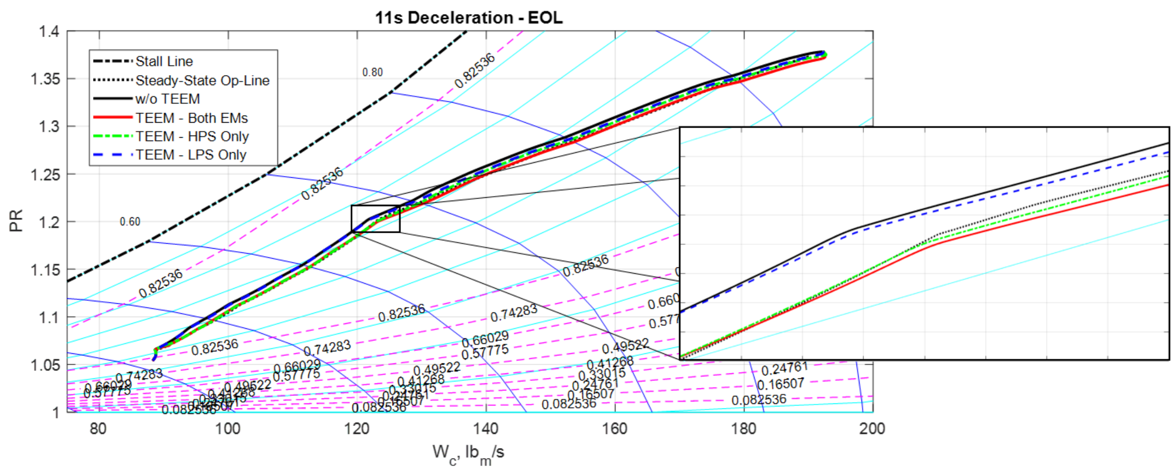

Figure 32. LPC map for an 11s deceleration transient with an EOL engine and the optimized w_f input profile. Transient lines are shown for the 3 TEEM strategies with 150hp of power transfer, injection, or extraction.

Acknowledgments

The authors would like to acknowledge the Transformational Tools and Technologies (TTT) project under the NASA Aeronautics Research Mission Directorate (ARMD) that has supported this work.

References

[1] Fuller, J., Kumar, A., and Millar, R., "Adaptive Model Based Control of Aircraft Propulsion Systems: Status and Outlook for Naval Aviation Applications," GT2006-90241, ASME Turbo Expo, Barcelona, Spain, 2006.

[2] Philpot, M., "Practical Consideration In Designing the Engine Cycle," Defense Technical Information Center, 1992.

[3] Spakovszky, Z., "Instabilities Everywhere! Hard Problems in Aero-Engines," GT2021-60864, ASME Turbo Expo, June, 2021.

[4] Kratz, J., "Transient Optimization of a Gas Turbine Engines", AIAA SciTech Forum, National Harbor, MD, January, 2023.

[5] Culley, D., Kratz, J., and Thomas, G., "Turbine Electrified Energy Management (TEEM) For Enabling More Efficient Engine Designs," AIAA Propulsion & Energy Forum, Cincinnati, OH. 2018.

[6] Jansen, R., Bowman, C., Jankovsky, A., Dyson, R., and Felder, J., "Overview of NASA Electrified Aircraft Propulsion Research for Large Subsonic Transports," AIAA Propulsion & Energy Forum, Atlanta, GA. 2017.

[7] Kratz, J., Culley, D., and Thomas, G., "A Control Strategy for Turbine Electrified Energy Management," AIAA Propulsion & Energy Forum, Indianapolis, IN. 2019.

[8] Kratz, J., Culley, D., and Thomas, G., "Evaluation of Electrical System Requirements for Implementing Turbine Electrified Energy Management," AIAA Propulsion & Energy Forum, Indianapolis, IN, 2019.

[9] Kratz, J., and Culley, D., "Enhancement of a Conceptual Hybrid Electric Tilt-Wing Propulsion System through Application of the Turbine Electrified Energy Management Concept," AIAA 2021-0875, AIAA SciTech Forum, Virtual Conference, 2021.

[10] Kratz, J., and Simon, D., "Failure Modes and Mitigation Strategies for a Turboelectric Aircraft Concept with Turbine Electrified Energy Management," AIAA SciTech Forum, San Diego, CA. 2022.

[11] Kratz, J., Connolly, J., Amthor, A., Buescher, H., Bianco, S., and Culley, D., "Turbine Electrified Energy Management for Single Aisle Aircraft," IEEE/AIAA Electric Aircraft Technologies Symposium, Anaheim, CA. 2022.

[12] Seok, J., Kolmanovsky, I., and Girard, A., "Coordinated Model Predictive Control of Aircraft Gas Turbine Engine and Power System," AIAA Journal of Guidance, Control, and Dynamics, Vol. 40, No. 10, October, 2017.

[13] Chapman, J., Litt, J., "Control Design for an Advanced Geared Turbofan Engine," AIAA Joint AIAA/ ASME/SAE/ASEE Joint Propulsion Conference, Atlanta, GA, 2017.

[14] May, R.D., Csank, J., Lavelle, T.M., Litt, J. S., and Guo, T.-H., "A High-Fidelity Simulation of a Generic Commercial Aircraft Engine and Controller," Proceedings of the 46th AIAA/ASME/SAE/ASEE Joint Propulsion Conference, AIAA-2010- 6630, Nashville, TN, July 2010.

[15] Chapman, J., Lavelle, T., May, R., Litt, J., and Guo, T.-H., "Toolbox for the Modeling and Analysis of Thermodynamic Systems (T-MATS) User's Guide," NASA TM-2014-216638, 2014.